Проблемы холодной темной материи как главного гравитирующего вещества

Сильченко О.К., ГАИШ МГУ

Эволюция крупномасштабной структуры: темная материя - ХОЛОДНАЯ

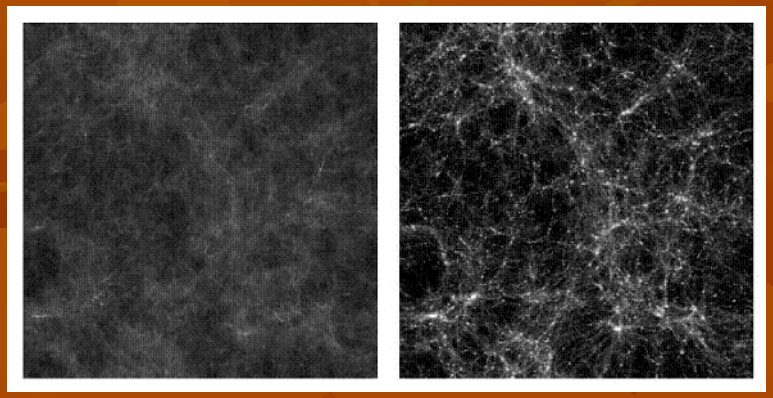

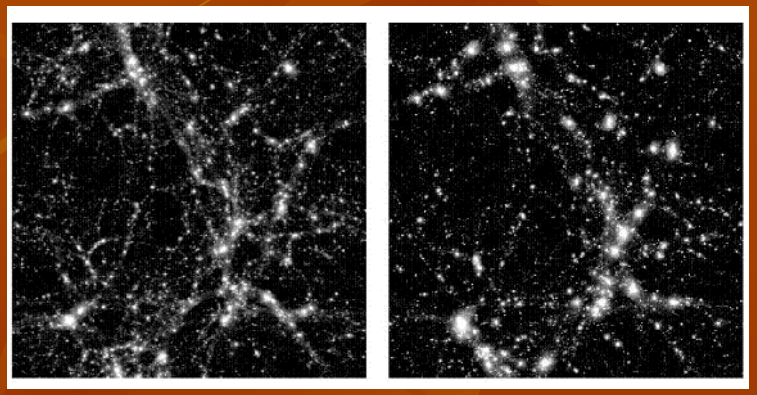

- Основной механизм – иерархическое скучивание материи под действием гравитационной неустойчивости
- Подбор параметров – чтобы получить правильную конечную картину к моменту z=0

Карликовые галактики на малых z: Comparison of the distribution function of line widths Vlos for galaxies in the Local Volume with theoretical predictions for the ΛCDM(left-hand panel) and the WDM models (right-hand panel, Planck cosmological parameters).

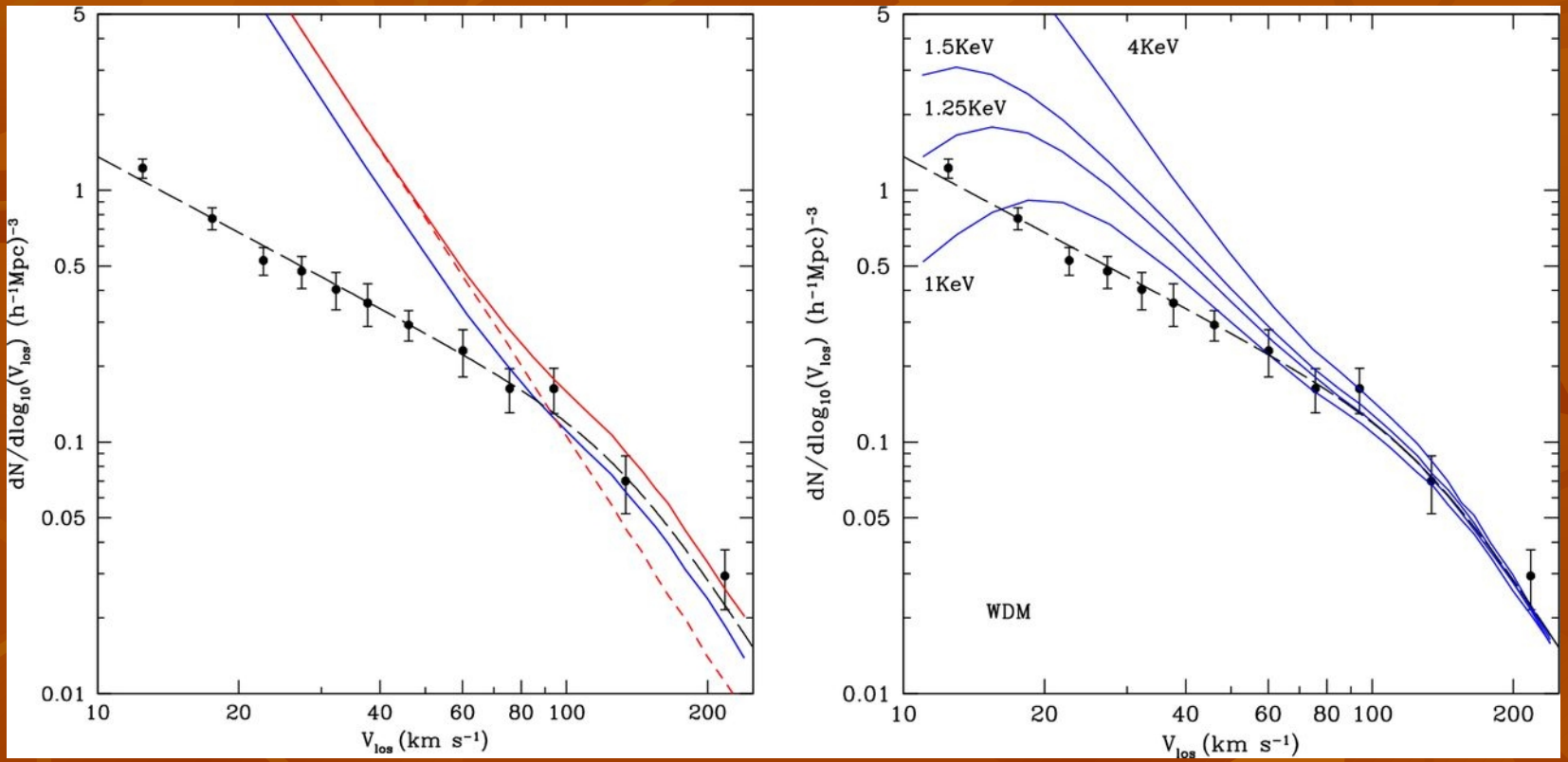

Anatoly Klypin et al. MNRAS 2015;454:1798-1810

MONTHLY NOTICES of the Royal Astronomical Society

Сравнение количества галактик разных масс на разных z с моделями

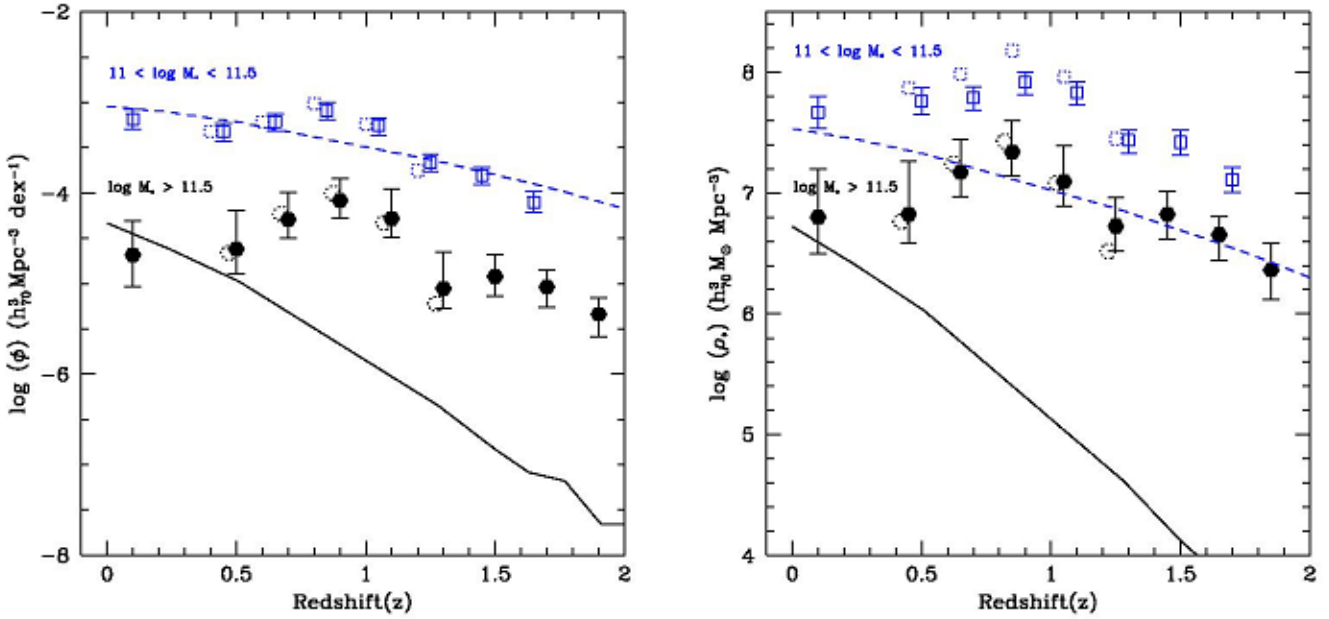

Figure 16. A comparison between our data and the models from the Millennium Simulation (e.g. De Lucia et al. 2006). The data shown are the same for the massive galaxy sample plotted in Fig. 4. The dashed line shows the predicted evolution in the number and stellar mass densities for $10^{11}\,M_\odot < M_* < 10^{11.5}\,M_\odot$ systems, while the solid line shows the same predictions for galaxies with stellar masses $M_* > 10^{11.5}\,M_\odot$. As can be seen, for the most part the simulated massive galaxies do not assembly quickly enough to match the observations.

Conselice et al. 2007

Downsizing!

Perez-Gonzalez et al. 2008

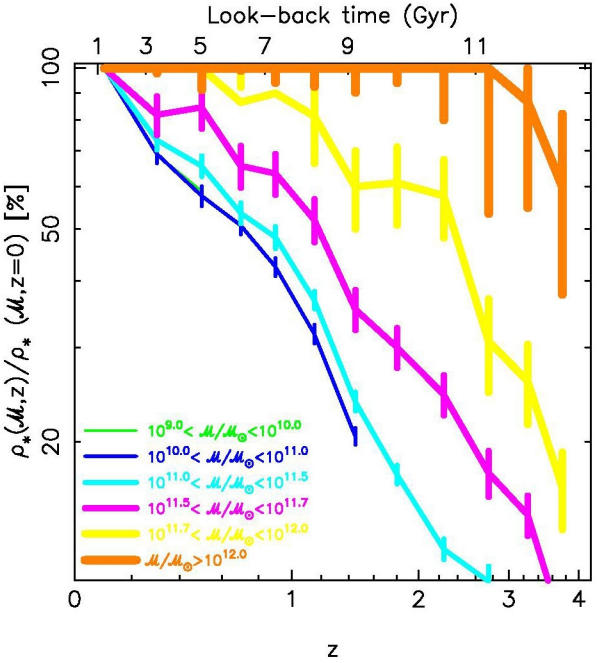

FIG. 6.— Fraction of the local stellar mass dens
sembled at a given redshift for several mass interv
referring to more massive systems). Only results fo
our 75% completeness level at each redshift are sho

Serjeant et al. 2008

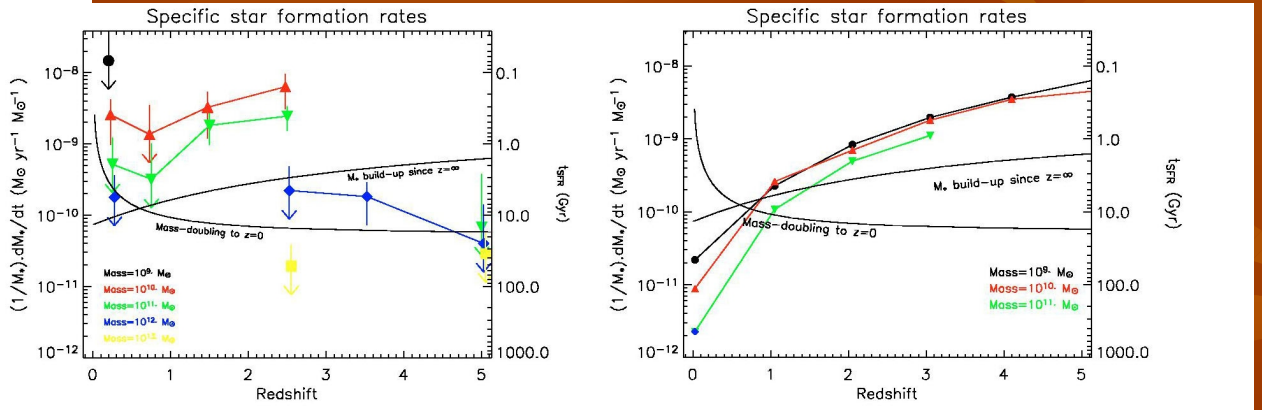

Figure 12. Left: SFR per unit galaxy mass, $(1/M)\ \mathrm{d}M/\mathrm{d}t$. This has dimensions of $[T]^{-1}$ and the corresponding star formation time-scales are given in the right-hand side ordinate. Symbols as in Fig. 10. Also plotted is the specific SFR required to double the stellar mass by $z = 0$ assuming a constant *specific* SFR, and the rate required to assemble the galaxy since the big bang assuming a constant SFR. Points lying above either line may be regarded as starbursting. Note that most of our detections can be regarded as starbursting. Right: corresponding predictions from the de Lucia et al. (2006) simulation. Note the obvious discrepancies with the observations.

Профили плотности темных гало: теория

- $\rho(r) = \rho_{cr}\,\delta_c / [(r/r_s)(1+r/r_s)^2]$

Navarro, Frenk, White (1996, 1997)

Профили плотности темной материи: наблюдения

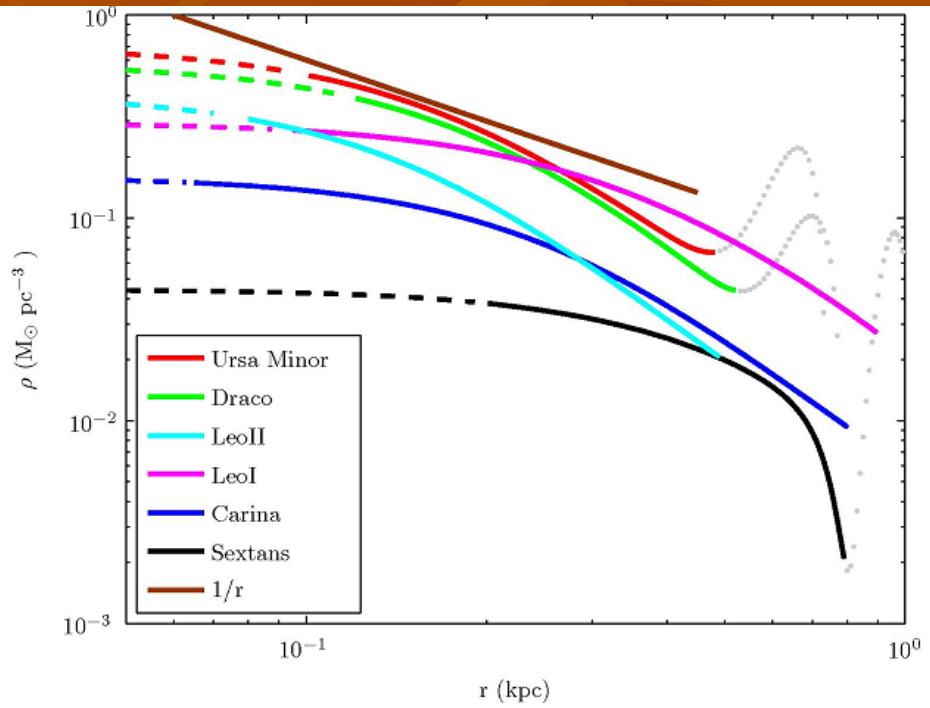

Fig. 4.— Derived inner mass distributions from isotropic Jeans' equation analyses for six dSph galaxies. The modelling is reliable in each case out to radii of log (r)kpc$\sim$ 0.5. The unphysical behaviour at larger radii is explained in the text. The general similarity of the inner mass profiles is striking, as is their shallow profile, and their similar central mass densities. Also shown is an r^{-1} density profile, predicted by many CDM numerical simulations (eg Navarro, Frenk & White 1997).

Обзор KMOS-3D: z=0.7-2.7, панорамная спектроскопия на VLT

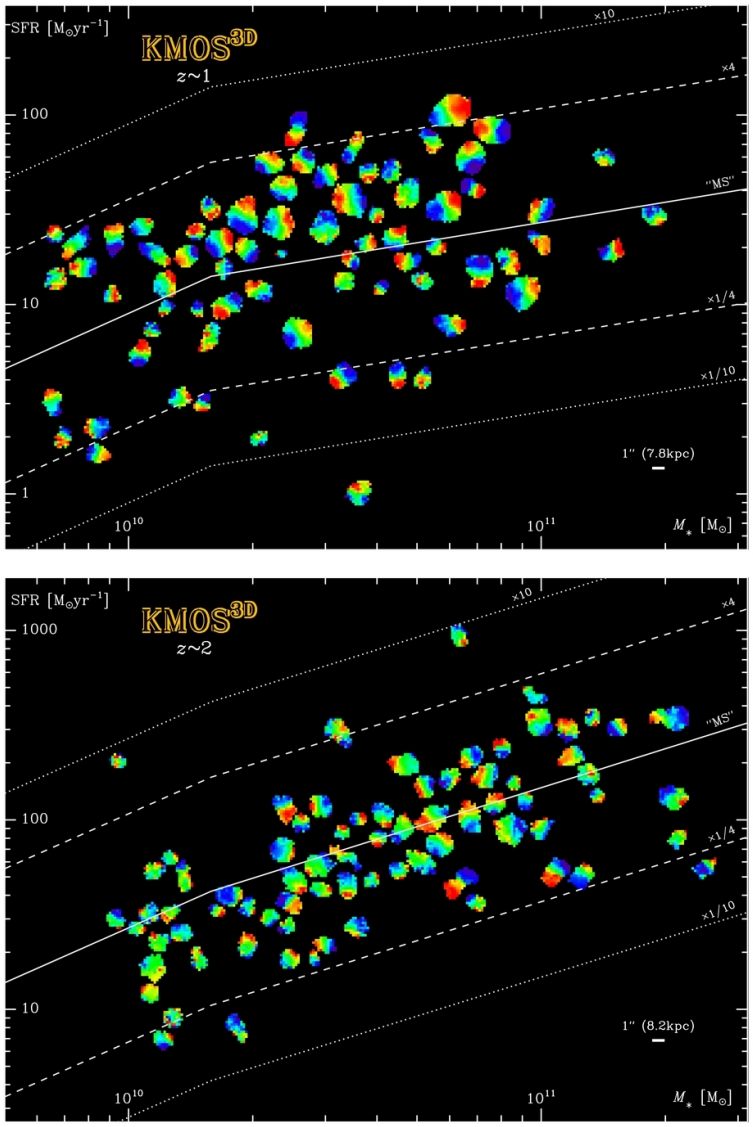

83% -Массивные, быстро вращающиеся диски, но ТОЛСТЫЕ И ГОРЯЧИЕ

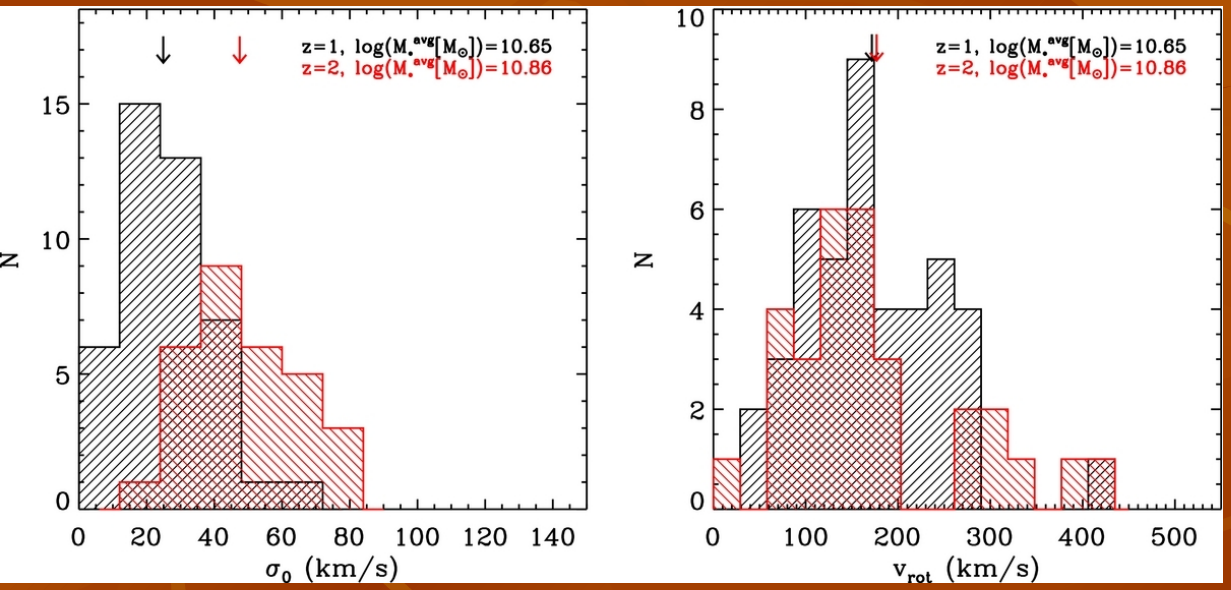

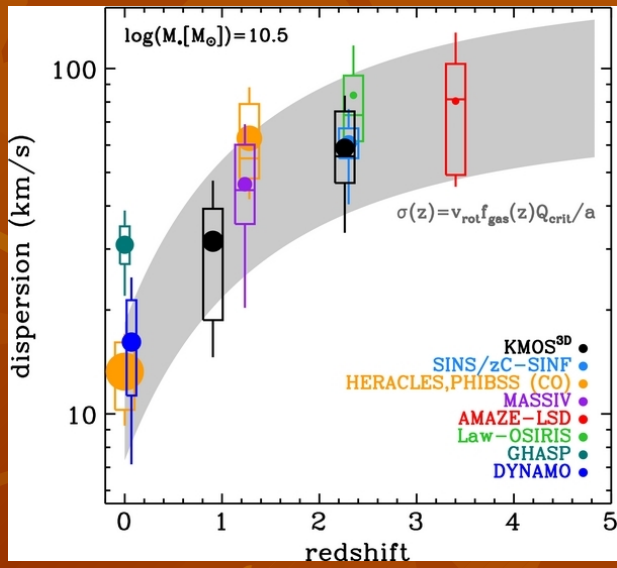

Wisnioski et al. 2015

FALLING OUTER ROTATION CURVES OF STAR-FORMING GALAXIES AT $0.6 \lesssim Z \lesssim 2.6$ PROBED WITH KMOS^{3D} AND SINS/ZC-SINF

Philipp Lang[1,2], Natascha M. Förster Schreiber[1], Reinhard Genzel[1,3,4], Stijn Wuyts[5], Emily Wisnioski[1], Alessandra Beifiori[1,6], Sirio Belli[1], Ralf Bender[1,6], Gabe Brammer[7], Andreas Burkert[1,6], Jeffrey Chan[1], Ric Davies[1], Matteo Fossati[1,6], Audrey Galametz[1], Sandesh K. Kulkarni[1], Dieter Lutz[1], J. Trevor Mendel[1], Ivelina G. Momcheva[7], Thorsten Naab[8], Erica J. Nelson[1], Roberto P. Saglia[1,6], Stella Seitz[6], Sandro Tacchella[10], Linda J. Tacconi[1], Ken-ichi Tadaki[1], Hannah Übler[1], Pieter G. van Dokkum[9], David J. Wilman[1,6]

[1] Max-Planck-Institut für extraterrestrische Physik, Giessenbachstrasse, D-85748 Garching, Germany

[2] Max-Planck-Institut für Astronomie, Königstuhl 17, D-69117 Heidelberg, Germany

[3] Department of Physics, Le Conte Hall, University of California, Berkeley, CA 94720, USA

[4] Department of Astronomy, New Campbell Hall, University of California, Berkeley, CA 94720, USA

[5] Department of Physics, University of Bath, Claverton Down, Bath, BA2 7AY, UK

[6] Universitäts-Sternwarte München, Scheinerstr. 1, München, D-81679, Germany

[7] Space Telescope Science Institute, 3700 San Martin Drive, Baltimore, MD 21218, USA

[8] Max-Planck-Institut für Astrophysik, Karl Schwarzschildstr. 1, D-85748 Garching, Germany

[9] Astronomy Department, Yale University, New Haven, CT 06511, USA

[10] Institute of Astronomy, Department of Physics, Eidgenössische Technische Hochschule, ETH Zürich, CH-8093, Switzerland

101 галактика между z=0.6 и z=2.6 – просуммировали!

Table 1. Median properties of the stacking sample.

Property	Median
z	1.52
$\log(M_*[M_\odot])$	10.61
$\log(M_{\rm baryonic} = M_* + M^a_{\rm gas})[M_\odot])$	10.87
$SFR\ [M_\odot/yr]$	41.9
$sSFR\ [Gyr^{-1}]$	1.20
R^b_e [kpc]	4.6
n^b	1.1

[a] Gas mass estimate based on empirical scaling relations.

[b] Intrinsic effective radius along the major axis and Sérsic index derived from H-band Sérsic fits.

Показатель Сersика =1 → экспоненциальные диски

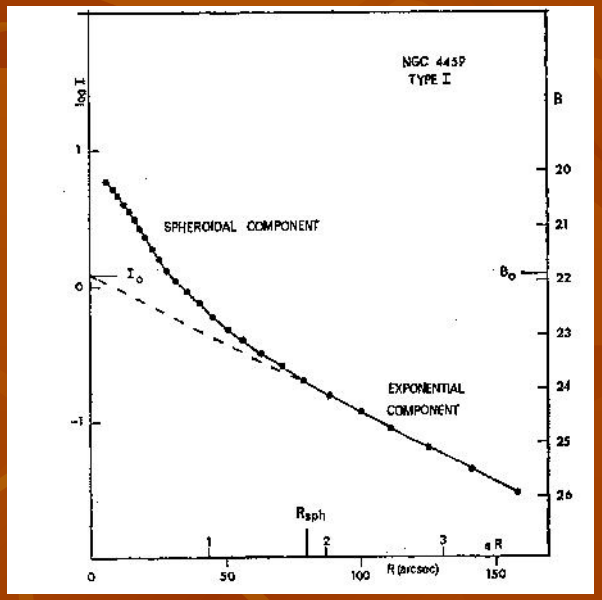

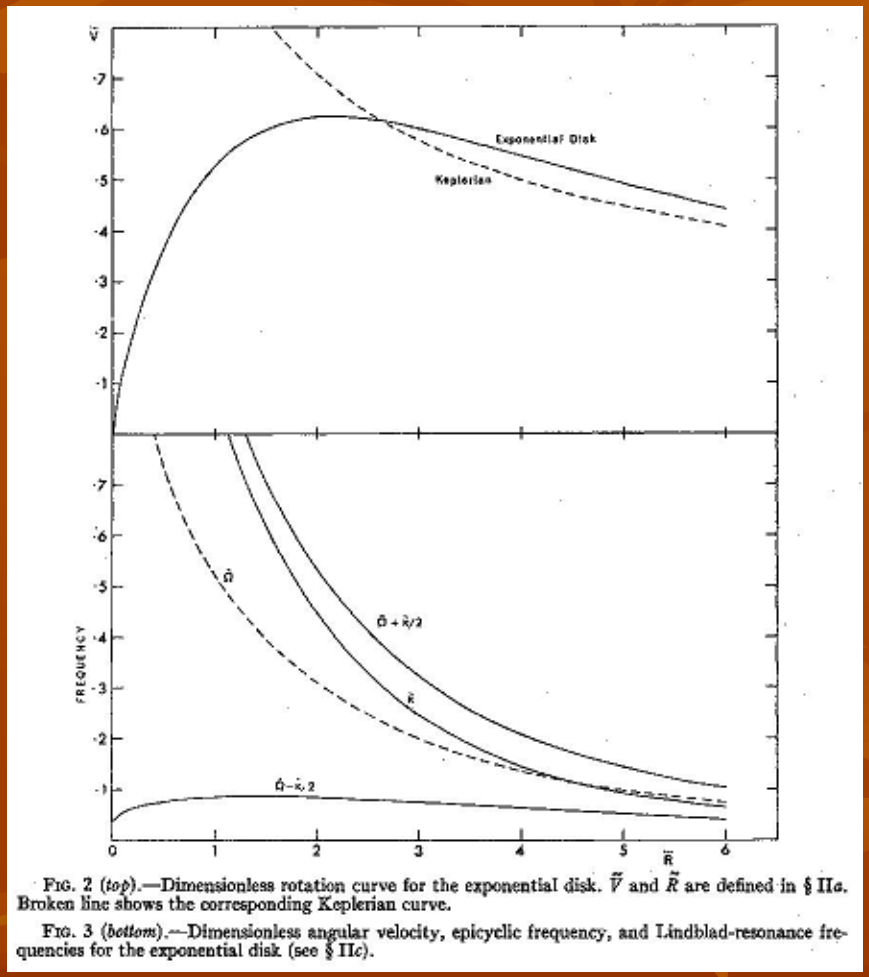

FIG. 2 (*top*).—Dimensionless rotation curve for the exponential disk. $\bar{V}$ and $\bar{R}$ are defined in § IIa. Broken line shows the corresponding Keplerian curve.

FIG. 3 (*bottom*).—Dimensionless angular velocity, epicyclic frequency, and Lindblad-resonance frequencies for the exponential disk (see § IIc).

… вписали в кривую вращения ионизованного газа модель экспоненциального диска

the noise cube associated with each data cube. Once we have constructed a rotation curve for each galaxy, we determine its observed amplitude and extent by fitting a Freeman exponential disk model of the form:

$$v_{\rm disk}(r) = \frac{r}{r_d}\sqrt{\pi G \Sigma_0 r_d [I_0 K_0 - I_1 K_1]}, \quad (1)$$

where r_d is the radial scale-length of the exponential disk, corresponding to $r_d = R_{\rm e}/1.68$. Σ_0 is the central mass surface density of the disk, and I_n and K_n denote the modified Bessel functions of the first and second kind (Freeman 1970). In the fitting, we leave r_d and Σ_0 as free parameters. Before fitting, the Freeman disk model is convolved with a 1D Gaussian of FWHM corresponding to the PSF associated with each galaxy. After the fit has converged, we determine the maximum observed velocity ($V_{\rm max}$) and the radius of the peak ($R_{\rm turn}$) from the model. In the right panels of Figure 2, rotation curves of two examples are shown together with the respective fit.

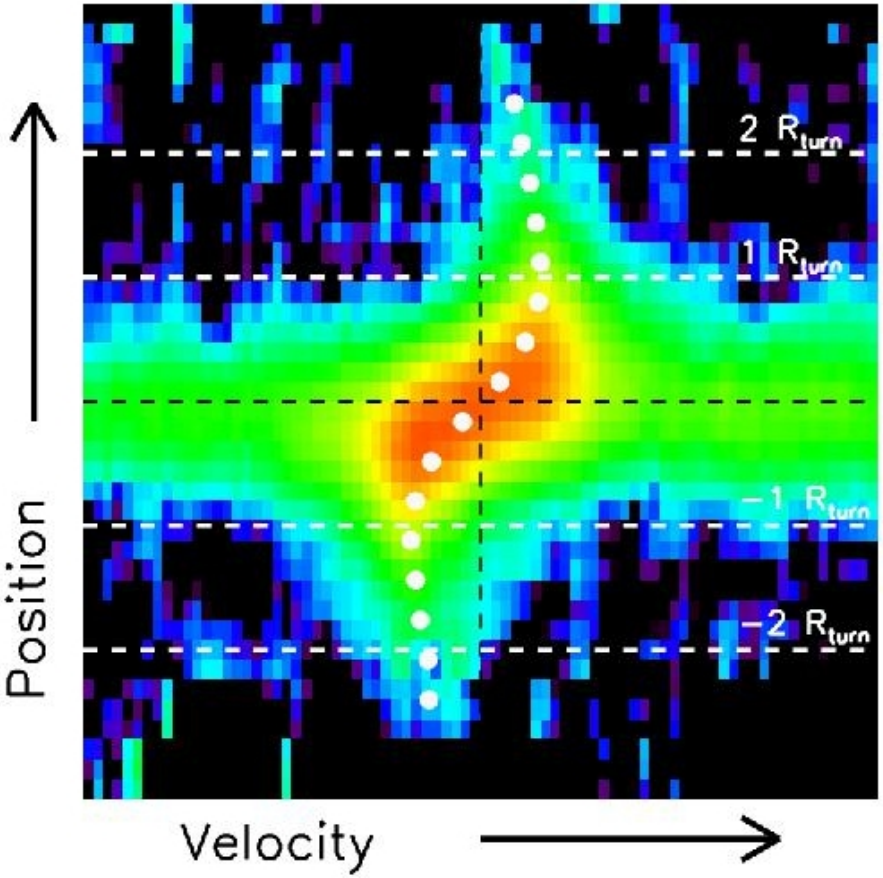

Figure 3. Final stacked pv diagram shown in logarithmic color scaling. The zero positions in velocity and radius are marked as black lines, and the radial position of $1R_{\rm turn}$ and $2R_{\rm turn}$ are marked as white dashed horizontal lines. The white symbols

Результаты

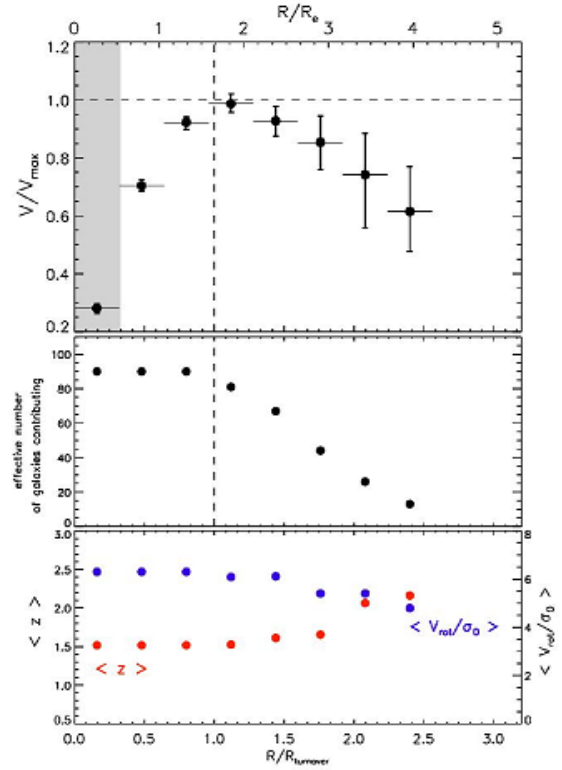

Figure 5. Top: Stacked rotation curve (black dots) plotted in units of normalized velocity (V/V_{max}), normalized radius (R/R_{turn}), and intrinsic effective radius (R/R_e). The error bars are derived from bootstrapping and include both sample variance as well as RMS noise in the spectra. The shaded area marks the half-light beam size of the average PSF observed for our sample. Middle: Effective number of galaxies contributing to the stack, accounting for masking out noisy pixels in the pv diagrams. The decrease in the number of contributing galaxies with increasing radius is driven by FOV limitations. Bottom: Median redshift and V_{rot}/σ_0 of contributing galaxies for a given radial bin.

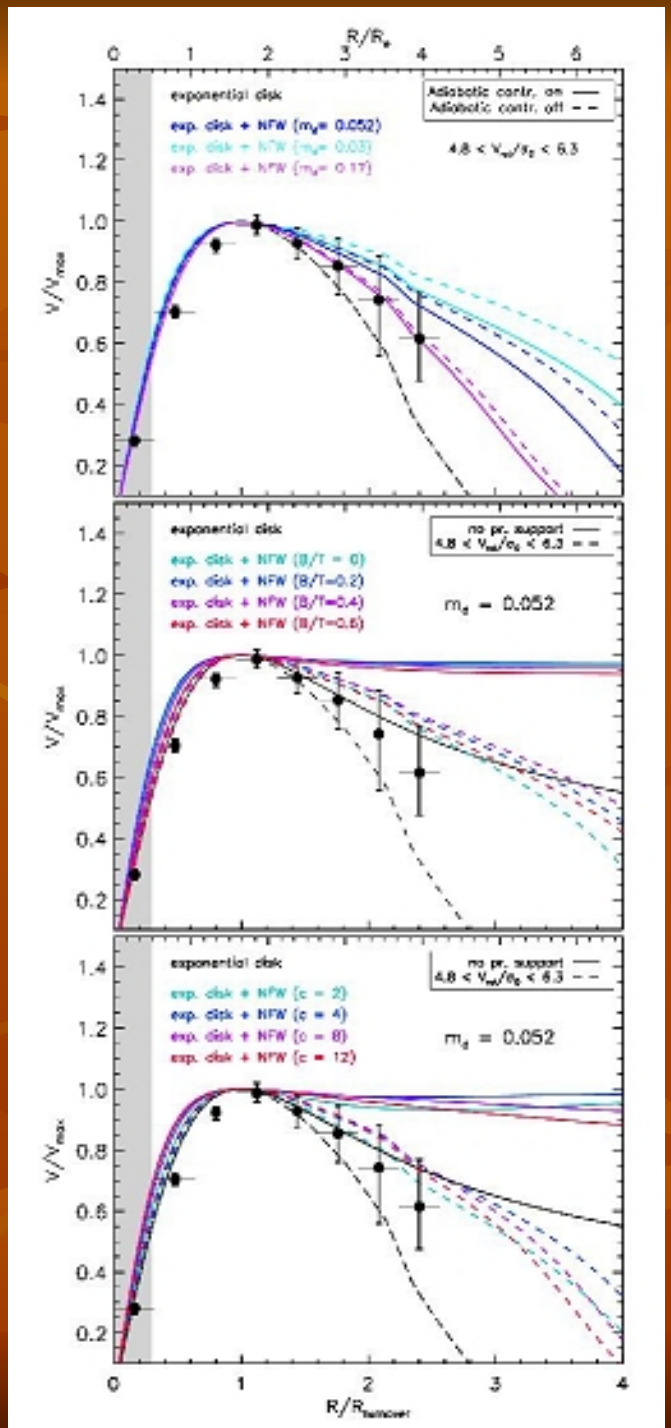

Главный результат – темное гало НЕ чувствуется (но подразумевается…)

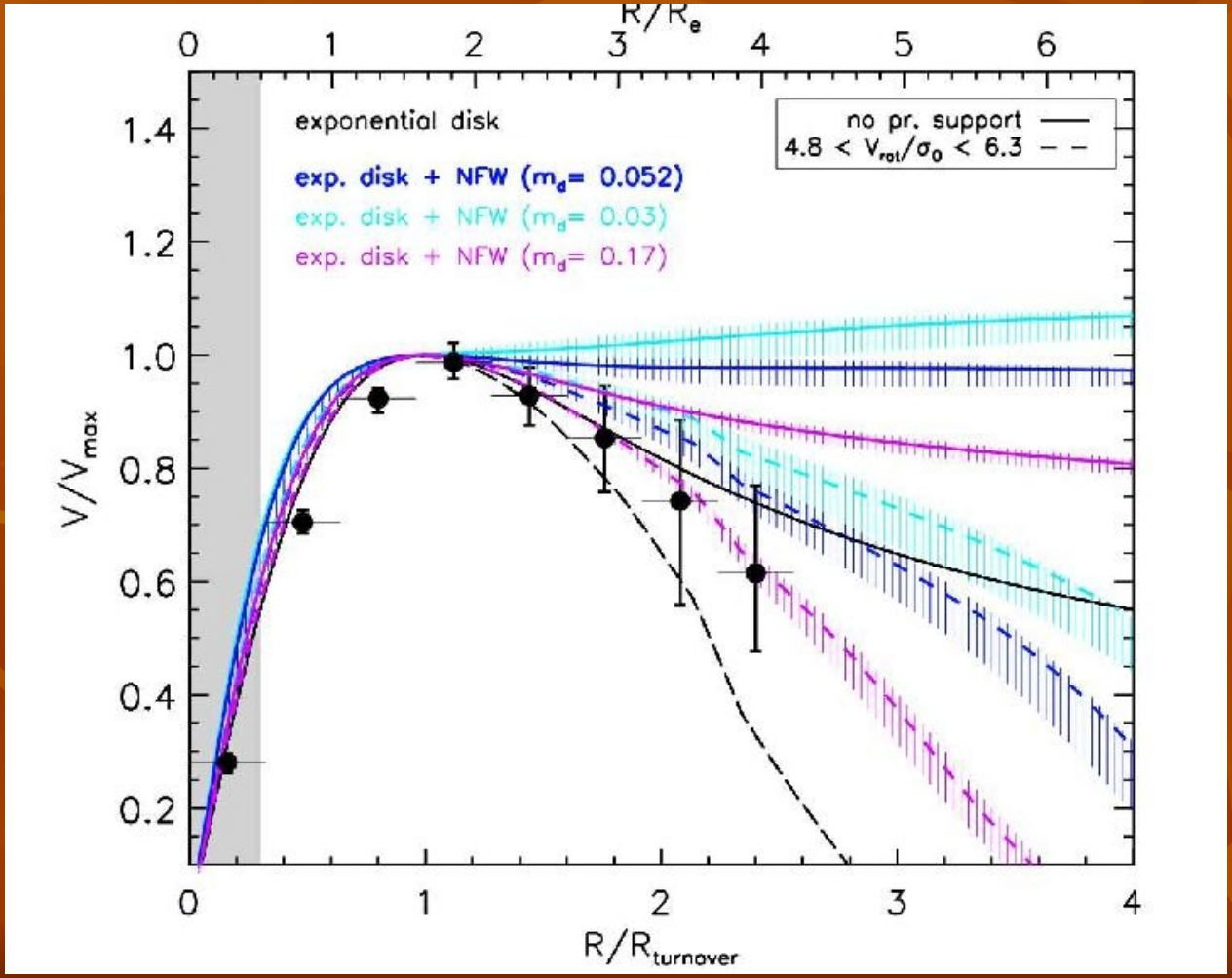

Genzel et al.: Nature!

Strongly baryon-dominated disk galaxies at the peak of galaxy formation ten billion years ago†

R.Genzel[1,2*], N.M. Förster Schreiber[1*], H.Übler[1], P.Lang[1], T.Naab[3], R.Bender[4,1], L.J.Tacconi[1], E.Wisnioski[1], S.Wuyts[1,5], T.Alexander[6], A. Beifiori[4,1], S.Belli[1], G. Brammer[7], A.Burkert[3,1], C.M.Carollo[8], J. Chan[1], R.Davies[1], M. Fossati[1,4], A.Galametz[1,4], S.Genel[9], O.Gerhard[1], D.Lutz[1], J.T. Mendel[1,4], I.Momcheva[10], E.J.Nelson[1,10], A.Renzini[11], R.Saglia[1,4], A.Sternberg[12], S.Tacchella[8], K.Tadaki[1] & D.Wilman[4,1]

[1]*Max-Planck-Institut für extraterrestrische Physik (MPE), Giessenbachstr.1, 85748 Garching, Germany (genzel@mpe.mpg.de, forster@mpe.mpg.de)*
[2]*Departments of Physics and Astronomy, University of California, 94720 Berkeley, USA*
[3]*Max-Planck Institute for Astrophysics, Karl Schwarzschildstrasse 1, D-85748 Garching, Germany*
[4]*Universitäts-Sternwarte Ludwig-Maximilians-Universität (USM), Scheinerstr. 1, München, D-81679, Germany*
[5]*Department of Physics, University of Bath, Claverton Down, Bath, BA2 7AY, United Kingdom*
[6]*Dept of Particle Physics & Astrophysics, Faculty of Physics, The Weizmann Institute of Science, POB 26, Rehovot 76100, Israel*
[7] *Space Telescope Science Institute, Baltimore, MD 21218, USA*
[8]*Institute of Astronomy, Department of Physics, Eidgenössische Technische Hochschule, ETH Zürich, CH-8093, Switzerland*
[9]*Center for Computational Astrophysics, 160 Fifth Avenue, New York, NY 10010, USA*
[10]*Department of Astronomy, Yale University, 260 Whitney Avenue, New Haven, CT 06511, USA*
[11]*Osservatorio Astronomico di Padova, Vicolo dell'Osservatorio 5, Padova, I-35122, Italy*
[12]*School of Physics and Astronomy, Tel Aviv University, Tel Aviv 69978, Israel*

Выборка

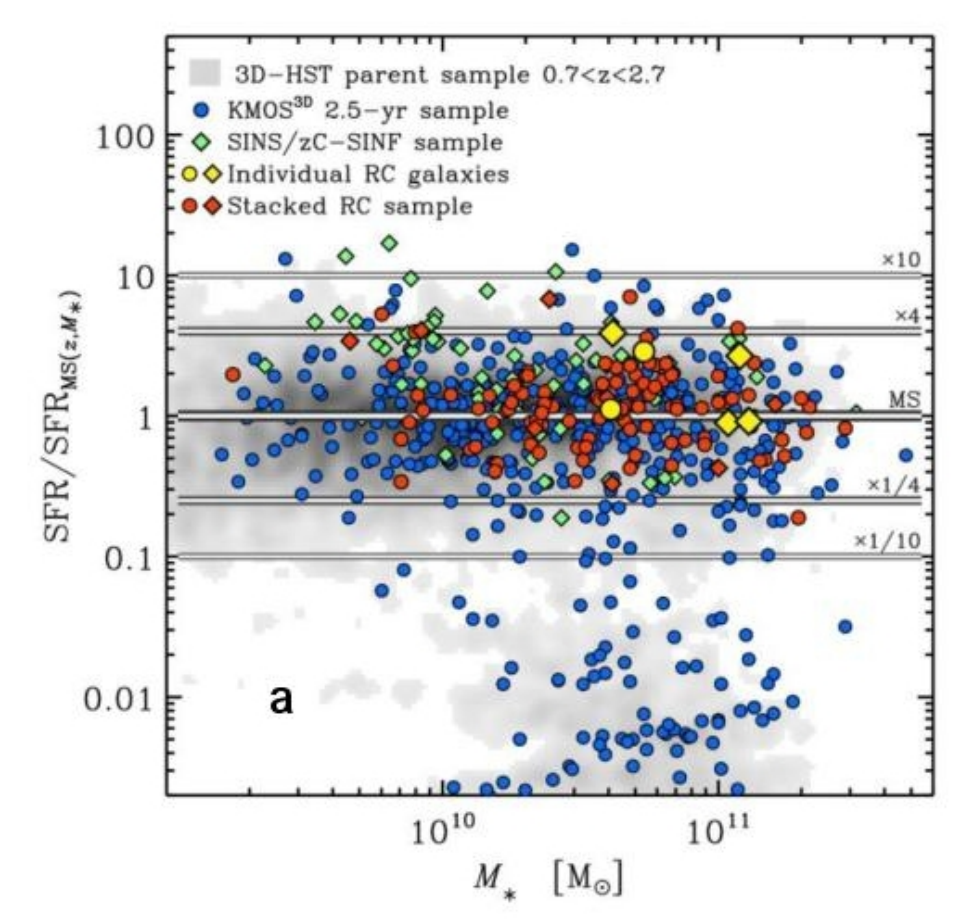
3D-HST parent sample 0.7<z<2.7
KMOS3D 2.5-yr sample
SINS/zC-SINF sample
Individual RC galaxies
Stacked RC sample
×10
×4
MS
×1/4
×1/10
a
100
10
1
0.1
0.01
SFR/SFR_MS(z,M*)
10^10
10^11
M* [M⊙]

Измерения

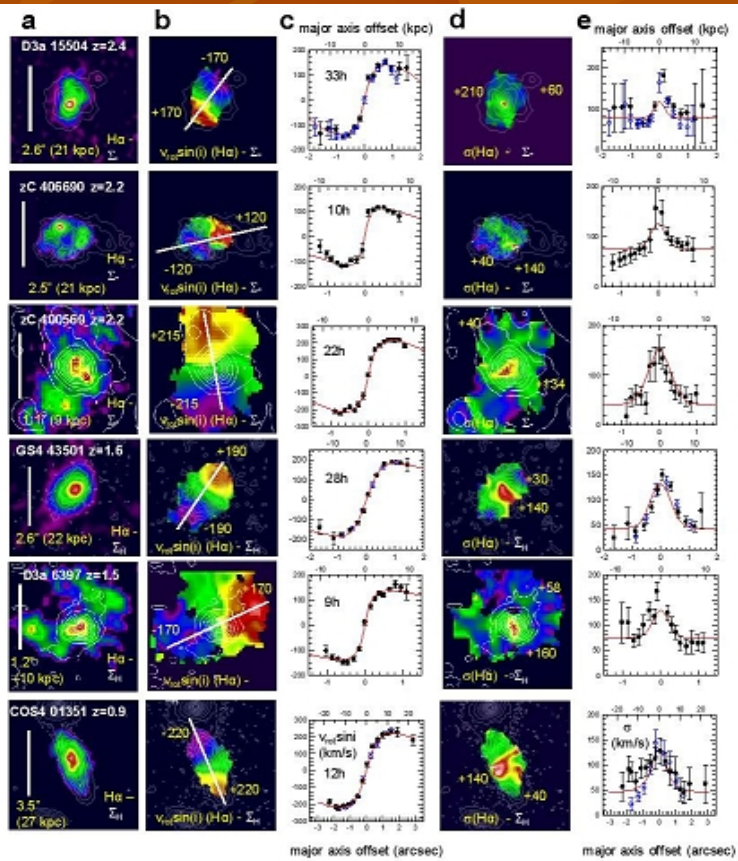

Figure 1. Hα gas dynamics from KMOS and SINFONI in six massive star-forming galaxies. The galaxies have redshifts between z=0.9 and 2.4. KMOS provides seeing-limited data (FWHM ~0.6"), and SINFONI allows both seeing-limited, and adaptive optics assisted observations (FWHM ~0.2"). For each galaxy column (a) shows the distribution of the integrated Hα line surface brightness (with a linear colour scale), superposed on white contours of the stellar surface density (Σ_*) or the H-band continuum surface brightness (Σ_H) (square root scaling). The vertical white bar denotes the 01351 and GS4 53501 we show both SINFONI (black filled circles) and KMOS (open blue circles) data sets, for D3a 15504 we show SINFONI data sets at 0.2" (black) and 0.5" (blue) resolution. Red continuous lines denote the best-fit dynamical model, constructed from a combination of a central compact bulge, an exponential disk and an NFW halo without adiabatic contraction, with a concentration of c=4 at z~2 and c=6.5 at z~1. For the modelling of the disk rotation, we also take into account the asymmetric drift correction inferred from the velocity dispersion curves ((d)-(e)[14]). Columns (d) and (e)

Еще измерения

Table 1. Physical Parameters of Observed Star-Forming Galaxies

	COS4 01351	D3a 6397	GS4 43501	zC 406690	zC 400569	D3a 15504
redshift	0.854	1.500	1.613	2.196	2.242	2.383
kpc/arcsec	7.68	8.46	8.47	8.26	8.23	8.14
Priors:						
M_* (10^{11} $M_\odot$)	0.54±0.16	1.2±0.37	0.41±0.12	0.42±0.12	1.2±0.37	1.1±0.34
M_{baryon}(gas+stars) (10^{11} $M_\odot$)	0.9±0.5	2.3±1.1	0.75±0.37	1.4±0.7	2.5±1.2	2.0±1.0
H-band $R_{1/2}$ (kpc)	8.6±1.3	5.9±0.8	4.9±0.7	5.5±1	4±2	6.3±1
inclination (°)	75±5	30±5	62±5	25±12	45±10	34±5
dark matter concentration parameter c	6.8	5	5	4	4	4
Fit parameters:						
$v_c(R_{1/2})$ (km/s)[a]	276	310	257	301	364	299
$R_{1/2}(n=1)$ (kpc)	7.3	7.4	4.9	5.5	3.3	6
σ_0 (km/s)	39	73	39	74	34	76
M_{baryon}(gas+stars, including bulge) (10^{11} $M_\odot$)	1.7	2.3	1.0	1.7	1.7	2.1
M_{bulge}/M_{baryon}	0.2	0.35	0.4	0.6	0.37	0.15
$f_{DM}(R_{1/2})=(v_{DM}/v_c)^2\|_{R=R1/2}$[b]	0.21 (±0.1)	0.17 (<0.38)	0.19 (±0.09)	0.0 (<0.08)	0.0 (<0.07)	0.12 (<0.26)

[a] Total circular velocity at the half-light radius (rest-frame optical) $R_{1/2}$, including bulge, exponential disk (n=1) and dark matter, and corrected for asymmetric drift: $v_c(R)^2=v_{rot}(R)^2+3.36\ \sigma_0^2\times (R/R_{1/2})|_{n=1.}$

[b] Ratio of dark matter to total mass at the half-light radius of the optical light, $f_{DM}(R_{1/2})=(v_{DM}/v_c)^2{}_{R=R1/2}$, with numbers in the parentheses giving the ±2 rms ($\delta\chi^2=4$, ~95% probability) uncertainties, or upper limits. We use an NFW halo of concentration parameter c, and no adiabatic contraction.

Главный результат: отсутствие темной материи – признак раннего типа галактики?

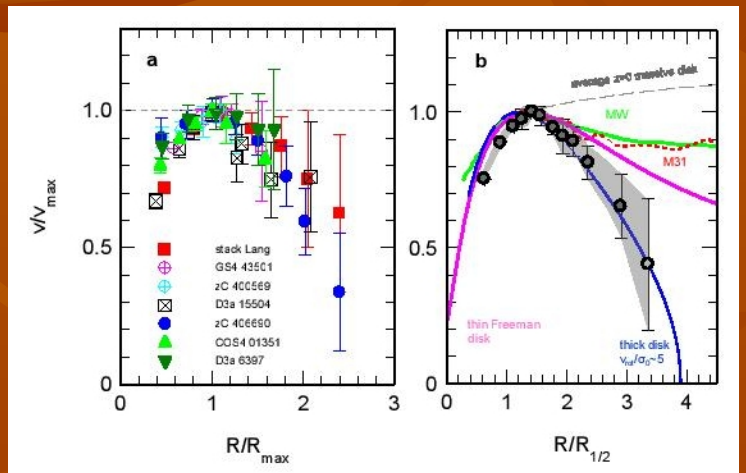

Figure 2. Normalized rotation curves. (a): The various symbols denote the folded and binned rotation curve data for the six galaxies in Figure 1, combined with the stacked rotation curve of 97 z=0.6-2.6 star-forming galaxies[18] (Methods). For all rotation curves we averaged data points located symmetrically on either side of the dynamical centres, and plot the rotation velocities and radii normalized to their maximum values. Error bars are ±1 rms. (**b**): The black data points

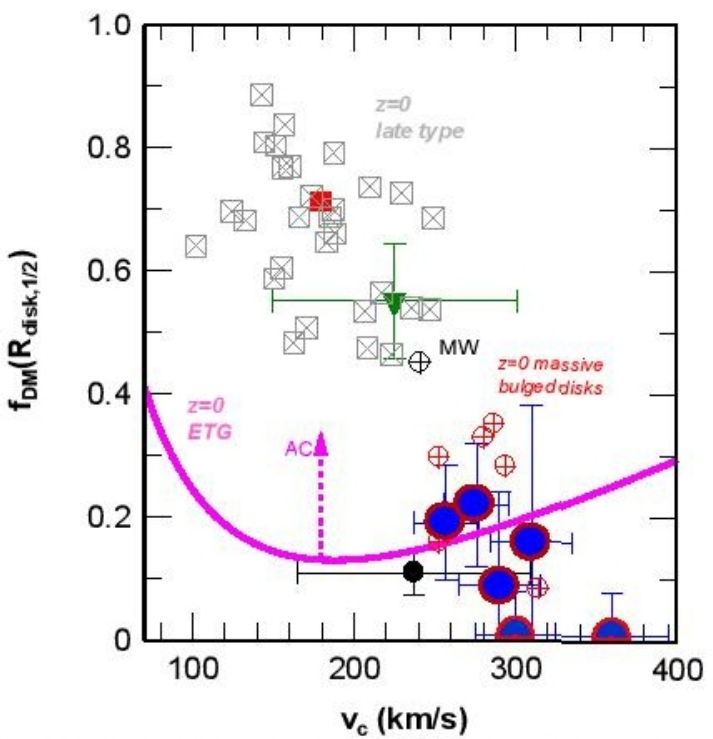

Figure 3. Dark matter fractions. Dark matter fractions from different methods are listed as a function of the circular velocity of the disk, at the half mass/light radius of the disk, for galaxies in the current Universe and ~10 Gyr ago. The large blue circles with red outlines indicate the dark matter fractions derived from the outer-disk rotation curves of the six high-z disks presented in this paper (Table 1), along with the ±2 rms

Выводы и спекуляции:

- На z=2 (10 млрд лет назад) в дисковых галактиках в пределах оптического радиуса доминируют барионы – в среднем до 90% общей динамической массы.
- С уменьшением z – с ходом эволюции Вселенной – доля барионов внутри оптического радиуса дисковых галактик ПЛАВНО падает.
- А на z=0 в пределах оптического радиуса барионы доминируют только в массивных галактиках ранних типов – РОДСТВЕННАЯ СВЯЗЬ? ЭФФЕКТ МАССЫ? ДРУГАЯ ПРИРОДА СОВРЕМЕННОГО ЗВЕЗДООБРАЗОВАНИЯ?